



Comparison of Gd-L X-rays RYIED and proton-NMRD

M.A. Reis^(a), P.C. Chaves^(a), A. Taborda^(c), A. Carvalho^(b)

(a) ITN, EN10 Sacavém, Apartado 21, 2686-953 SACAVÉM, PORTUGAL

(b) ESTeSL, Av. D. João II, lote 4.69.01, 1990-096 Lisboa, PORTUGAL

(c) IST, Av. Rovisco Pais, 1, 1049-001 Lisboa, PORTUGAL

Abstract. In previous works, it was shown that, for W under proton irradiation, the x-ray relative yields were dependent on the energy of the irradiation ion beam. This was then named Relative Yield Ion Energy Dependence (RYIED) and was seen both for the L [1] as well as for the K shell x-rays[2]. In the present work, this effect is further explored and comparisons are made to data originating from a totally different analytical technique, namely the analysis of the proton longitudinal relaxation time dependence on the Larmor frequency (proton-NMRD). This technique when applied to water solutions of chelate of paramagnetic ions, provides information on the electronic configuration of the chelate, including the electrons surrounding the core ion. Experimental evidence related to RYIED effects strongly suggests an important connection between intensity ratio variation patterns and the electronic configuration where the emitting ion is embedded. This work focus on the L-shell x-ray lines of Gd and namely on the ratios of intensity of lines corresponding to transitions to the same sub-shell (LI, LII and LIII). Results are presented for three different Gd environments and for several proton beam irradiation energies between 0.7 and 1.95 MeV.

Keywords: Low energy PIXE, RYEID, proton-NMRD, transition rates, intensity ratios.

INTRODUCTION

In PIXE work it is usually assumed that the ratio between two x-ray lines of the same element is an atomic parameter independent of the chemical environment surrounding the emitting ion. That this in detail is not exactly the case, is also a well known fact, shown by several authors [1-10]. Some of these works even compare results to *ab initio* calculations[8,9]. Recently, effects due to an applied external magnetic field have also been reported on the fluorescence yield of LIII sub-shell of Gd, Dy, Hg and Pb by Demir [11]. In a PIXE experiment, the x-ray emitting ion is located in a condensed matter environment, and is therefore subjected to strong local magnetic and electric fields due to the surrounding electronic configuration. This fact is one of the main reasons for lacking of stability of the line ratios. Furthermore, it is important to realise that in parallel to the main process of ionization of the inner-shell, during the collision between the incident beam ions and the sample atoms, other secondary

processes take place such as multi-ionization, shake-off and polarization of atomic orbitals. In this communication it is shown that the intensity ratio between lines of the same sub-shell is not only dependent on the chemical environment of the x-ray emitting ion, but also on the ion beam energy. A parallel is then made towards nuclear magnetic resonance dispersion (NMRD) studies.

In NMRD longitudinal and transverse magnetic relaxation rates, T₁ and T₂ are measured for a broad range of Larmor frequencies (♦). The obtained T₁(♦) and T₂(♦) curves are then called nuclear magnetic relaxation dispersion curves. NMRD is particularly interesting in the case of paramagnetic systems. In this case, the proper simulation of the T₁(♦) and T₂(♦) curves, using adjustable parameters models, provides an important insight into the paramagnetic system environment [12], including also data relative to the paramagnetic center itself.

Assuming a formal resemblance between the static magnetic field intensity in NMRD and the ion beam

energy in RYIED, a second formal resemblance may be made between the $T_1(\diamond)$ curves in NMRD and the intensity ratio variation curves in RYIED. This formal resemblance (for the time being), takes us to believe that RYIED is indeed a strong candidate for an ion beam x-ray technique to study the electronic or chemical environment of a given atom.

MATERIALS AND METHODS

In other works [1,2,13], W and Mo were studied. In the present work, an element having different characteristics, namely an element allowing the measurement of the L shell as well as the K and the M shells x-rays, using the available equipment, was aimed at and Gd was selected. Gd is an important technological element, namely for biomedical applications, being used as paramagnetic contrast agent (CA) for nuclear magnetic resonance imaging (MRI), due mainly to its large magnetic moment[14].

Gd L-shell spectra were obtained using a 150 eV resolution LN-cooled Scirus Si(Li) detector from Gresham Scientific Instruments Lda. As irradiation targets, a Gd₂O₃ pellet, Gd₂O₃ 5nm particles dispersed on a polycarbonate membrane filter, and a GdDOTA pellet, were used. GdDOTA is a Gd chelate used in the production of MRI contrast agents. Pure materials, namely 99.99% pure Gd₂O₃ powder from Alfa Aesar®, and 99.9% pure Gd₂O₃ nano particles and 97.5% pure Gd-DOTA from Sigma-Aldrich Co., were used to avoid problems in data interpretation due to sample contamination. To further avoid problems due to the sample preparation, irradiation targets were made in glove chambers and in an inert dry atmosphere to prevent for sample degradation. Once ready, the samples were placed in the irradiation chamber under vacuum, to assure that no degradation or contamination would arise from atmospheric exposure. The experimental facilities details can be found in a previous work [15]. Spectra were obtained for proton energies from 700 keV to 1450 keV in steps of 50 keV, and for 1700 keV and 1950 keV. Spectra deconvolution was carried out using the new DT2 program core, presented at this conference[16]. This includes a Bayesian inference algorithm by Barradas[16,17], for determination of the error levels associated to the fitted line areas.

RESULTS AND DISCUSSION

In fig.1 the ratios determined for lines of the same sub-shell are presented for $L\beta_2/L\alpha_1$ (both L_{III} transitions), $L\gamma_1/L\beta_1$ (both L_{II} transitions) and $L\beta_{3,4}L\gamma_2$ (both L_I transitions), for three different Gd

environments, and as function of the incident proton beam energy. It can be seen that the ratios variation curves are different for the three samples: the GdDOTA pellet, the Gd₂O₃ 5 nm particles dispersed on a filter and the Gd₂O₃ pellet.

FIGURE 1. Line intensity ratio curves for L_{III} , L_{II} and L_I sub-shell lines, top to bottom respectively. The experimental values are connected by a spine curve for easy reading of the plots.

It is here important to emphasise that the 5nm particles by being dispersed on a polycarbonate membrane can be seen as a thin film and therefore do not present any auto-absorption effects. This fact explains partially the difference between the Gd₂O₃ 5 nm particles and the Gd₂O₃ pellet in the topmost plot. In fact, the rising tendency of the $L\beta_2/L\alpha_1$ ratio for the Gd₂O₃ pellet can be explained by auto-absorption effects since the $L\beta_2$ line has a higher energy than the $L\alpha_1$, and therefore suffers less absorption when produced deeper in the target. The same reasoning can be applied to the difference in level between the Gd₂O₃ pellet and the 5 nm particles. Still, the difference in pattern cannot be explained in this way. The high statistics spectra collected (roughly 200 000 counts in the $L\alpha$ group) and the precision of the Bayesian inference algorithm, both play an important task here, allowing for differences to be significant since errors are below 5% in most cases. One very interesting feature which further supports the effectiveness of these results is the almost perfect match of the $L\beta_2/L\alpha_1$ ratio for the Gd₂O₃ 5 nm particles and the GdDOTA pellet from 700 keV up to 1150 keV, a total of nine points, and eighteen spectra. This feature, clearly seen directly from the spectra normalized to the $L\infty$ group, is amazing since we are comparing a pellet sample to a thin film sample. The size of the GdDOTA chelate molecule, similar to the size of the Gd nanoparticles can be speculated to be behind this result. This observation which also stresses more the difference to the Gd₂O₃ pellet in this range of energies.

The differences found in patterns culminate with the results for the $L\beta_{3,4}L\gamma_2$ ratio, where a difference of a factor of 2 can be observed between the Gd₂O₃ pellet and the Gd₂O₃ 5 nm particles for an energy of 1100 keV. In this $L\beta_{3,4}L\gamma_2$ ratio pattern, partial terms can also be observed. In fact, for Gd₂O₃ pellet and Gd₂O₃ 5 nm particles the patterns are similar up to 900 keV and not further, while Gd₂O₃ pellet and GdDOTA patterns are similar in the range from 1050 keV to 1250 keV. This leads to the conclusion that additive terms must be at stake here.

The NMRD case

NMR of water solutions of paramagnetic systems, measures the T_1 and T_2 for the water protons. These are strongly affected by the presence of a paramagnetic solute, due both to the magnetic center (the Gd in the case of Gd compounds) and to its surrounding environment (the DOTA chelate molecule, in the case of GdDOTA). In NMRD, the $T_1(\bullet)$ and $T_2(\bullet)$ curves are obtained as function of a broad range of static magnetic field values, expressed as proton Larmor frequencies (\bullet).

The most used description of proton nuclear relaxation in the presence of paramagnetic ions is the Solomon, Bloembergen and Morgan (SBM) theory [12]. In this theory the $1/T_1(\bullet)$ is expressed as function of the Larmor frequency and a set of parameters:

$$\frac{1}{T_1(\omega)} = F(\omega, param) \quad (1)$$

where $param = r_{IS}, \tau_R, \tau_M, T_{1e}, T_{2e}, \omega_S, S, \mu_{ef}, T$.

These parameters are: *i*) r_{IS} , the distance between the spin of the unpaired electrons and the water proton nuclear spin, *ii*) T_R , the complex (chelate plus active centre) rotation correlation time, *iii*) T_M , the water molecule mean residence time within the paramagnetic complex (although not strict, for most of the available complexes, only one molecule is present within the complex environment at any given moment), *iv*) T_{1e} and T_{2e} , the active center electrons longitudinal and transverse electronic relaxation times, *v*) ω_S , the active center electronic Larmor frequency, *vi*) S the active center electronic spin, *vii*) O_{ef} , the effective magnetic moment, $O_{ef} = g_e O_B \sqrt{J(J+1)}$ for lanthanides (where g_e and O_B are the Landé g -factor and the Bohr magneton respectively, and J is active center electronic total angular momentum), *viii*) T , is the solution temperature.

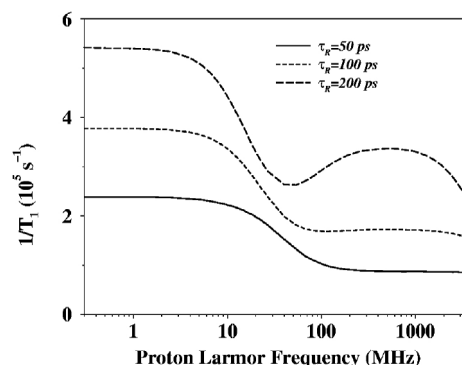


FIGURE 2. $1/T_1(\bullet)$ curves simulated for theoretical Gd^{3+} complexes in water solution, for three different rotation correlation times, the other parameters having the values presented in table 2.

Fig. 2 presents, as an example, $1/T_1(\bullet)$ curves for three different theoretical Gd^{3+} complexes ($S=7/2$), assuming that the single difference between them is the T_R , parameter. The sensitivity of the technique relative to this parameter is here clearly seen.

TABLE 2. Parameters used to generate the curve in Fig.2.

$\tau_R = 0.5, 1 \text{ and } 2 \times 10^{-10} \text{ s}$	$T_M = 1 \times 10^{-8} \text{ s}$
$S = 7/2$	$r_{IS} = 3.1 \times 10^{-10} \text{ m}$
$T = 298 \text{ K}$	$\mu_{ef} = 6.492 \times 10^{-23} \text{ JT}^{-1}$

CONCLUSIONS

It was shown that L-shell x-ray relative intensity is dependent upon the irradiation ion beam energy, even in the case of lines corresponding to transitions to the same L sub-shell. The patterns found are different for different emitting ion electronic environments, and the existence of additive terms can be speculated for. In the authors opinion, the results presented here point to the fact that RYIED should be seen as a new analytical technique in itself and, even if at the present stage of development, the similarity between the RYIED and NMRD curves may be seen as a simple coincidence, the fact that there is a formal resemblance to NMRD still persists. NMRD is a well established technique which provides insight into many parameters of paramagnetic complexes (just to mention the specific type of application presented in this communication) and, the theory behind NMRD is not simple and many different atomic and molecular parameters are at stake. It is therefore expectable that for RYIED, many parameters and much work is required before it becomes possible to generated theoretical curves like it

is currently possible in NMRD, still the results presented here seem promising enough for that work to look worthy. Furthermore, the resemblance between RYIED and NMRD, in this work assumed as just formal, may become more than that because it is reasonable to assume that many of the parameters required for RYIED will overlap those present actually in NMRD.

ACKNOWLEDGMENTS

This work is funded in the framework of project REEQ/377/FIS/2005 of the Fundação para a Ciência e a Tecnologia.

A word of acknowledgment is also due J.P. Leal for the support in using the glove box for samples preparation.

REFERENCES

1. M.A. Reis, P.C. Chaves, J.C. Soares, Nuclear Instruments and Methods in Physics Research, B229 (2005) 413-424.
2. P.C. Chaves, M.A. Reis, in Proceedings of the X Int. Conf. on PIXE and its Analytical Applications, Portorož, Slovenia, June 4-8, – IJS, LjubLjana 2004
3. S. Raj, H. C. Padhi, M. Polasik, Nuclear Instruments and Methods in Physics Research B 145 (1998) 485-491.
4. S. Raj, H. C. Padhi, M. Polasik, Nuclear Instruments and Methods in Physics Research B 155 (1999) 143-152.
5. S. Raj, H. C. Padhi, D. K. Basa, M. Polasik, F. Pawlowski, Nuclear Instruments and Methods in Physics Research B 152 (1999) 417-424.
6. S. Raj, H. C. Padhi, M. Polasik, Nuclear Instruments and Methods in Physics Research B 160 (2000) 443-448.
7. H.C. Padhi, Bhuinya, B.B. Dhal, Journal of Physics B: Atomic, Molecular and Optical. Physics 26 (1993) 4465-4469
8. F. Pawłowski, m. Polasik, S. Raj, H.C. Padhi, D. K. Basa, Nuclear Instruments and Methods in Physics Research B 195 (2002) 367-373
9. K. Jankowski, M. Polasik, Journal of Physics B: Atomic, Molecular and Optical. Physics 22 (1989) 2369-2376
10. K. Kawatsura, K. Ozawa, M. Terasawa, K. Komaki and F. Fujimoto, Nuclear Instruments and Methods in Physics Research B 75 (1993) 28-31.
11. D. Demir, Y. Sahin, Nuclear Instruments and Methods in Physics Research B 254 (2007) 43–48
12. L. Helm, Progress in Nuclear Magnetic Resonance Spectroscopy, 49 (2006) 45-64
13. P.C. Chaves, M. Kavčič, M.A. Reis, this conference PI-3
14. The Chemistry of Contrast Agents in Medical Magnetic Resonance Imaging, A.E. Merbach, É. Tóth (Eds), Wiley & Sons (2001)
15. M.A. Reis, P.C. Chaves, V. Corregidor, N.P. Barradas, E. Alves, F. Dimroth And A.W. Bett, X-ray Spectrometry 34 (2005) 372-375
16. M.A. Reis, P.C. Chaves, C. Pascual-Izarra, L.C. Alves, N. P. Barrada, this conference, PII-1
17. Barradas private communication (2006)